Biochemical Engineering Journal 198 (2023) 109044

Contents lists available at ScienceDirect

Biochemical Engineering Journal

journal homepage: www.elsevier.com/locate/bej

Regular article

Optimization and kinetic analysis of untreated brewers' spent grain saccharification process via enzymatic hydrolysis

Leonardo Sibono [a], Stefania Tronci [a], Ron Hajrizaj [b], Knud V. Christensen [b], Massimiliano Errico [b,*], Massimiliano Grosso [a]

[a] Università degli Studi di Cagliari, Dipartimento di Ingegneria Meccanica, Chimica e dei Materiali, Cagliari I-9123, Italy
[b] University of Southern Denmark, Faculty of Engineering, Department of Green Technology, Odense M 5230, Denmark

ARTICLE INFO

Keywords:
Lignocellulosic biomass
Enzymatic hydrolysis
Chrastil's model
Response surface methodology
Enzymatic kinetics

ABSTRACT

The enzymatic hydrolysis of dried brewers' spent grain without being pretreated was investigated in this work. The enzymatic hydrolysis experiments were carried out using Cellic ® CTec2 as enzymatic complex and the glucose yield was optimized with respect to temperature, solid loading and enzyme loading. The optimization of enzymatic hydrolysis obtained through the response surface methodology was validated experimentally resulting in a glucose yield of 11.71 ± 0.09 $g_{glucose} g_{DM}^{-1}$ at 48.6 °C, 6.7 % w/w biomass loading, and 0.22 mL g_{DM}^{-1} as enzyme concentration. The glucose yield obtained corresponds to 44 % of the theoretical one. The temporal profile of glucose concentration was modeled by using the Chrastil's model, and by a modified version of its classical formulation. The models were compared with respect to the fit goodness and precision of parameter estimation. Even if both models were able to properly describe the transient behavior, the proposed modified Chrastil's model provided a more precise parameter estimation compared to the classical one.

1. Introduction

Lignocellulosic biomasses represent a promising, renewable, widely available, and cheap material from which high-adding-value compounds and platform chemicals can be obtained. Particularly, brewers' spent grain (BSG) is the most abundant by-product of the brewing industry with a generation rate of 20 kg per 100 L of beer produced [1]. The estimated worldwide beer production of 1.86 billion hectoliters [2] makes BSG a widely available by-product whose valorization appears essential to move towards sustainable breweries.

BSG is the solid residue, mainly constituted by the barley grain husks, obtained from the lautering stage where the wort is recovered. In terms of composition, BSG is composed of 15–25 % cellulose, a homopolymer consisting of glucose monomers joined by β-1,4-glycosidic bonds, along with 20–40 % hemicellulose, a polymer made of pentose sugars, predominantly xylose and arabinose, and 10–20 % lignin, a polyphenolic macromolecule. The rest is composed of proteins and extractives [3]. Currently, BSG is mainly used as animal feed with an associate value of 13.95 €/ton [4,5]. Due to its composition, there is a growing interest in using BSG as a raw material for the recovery of high-value fractions and components. As simple sugars are precursors for several industrial-relevant products, the depolymerization of the polysaccharide fraction is a possible route for its valorization [6]. However, due to its fibrous nature, several complex steps are typically required to extract a significant quantity of sugars from BSG. It is expected that producing fermentable sugars by means of hydrolysis followed by alcoholic fermentation through ethanologenic microorganisms will increase the BSG valorization potential [7]. In most cases, enzymatic hydrolysis is employed to convert cellulose into glucose. As cellulose in lignocellulosic biomasses like BSG is physically linked with hemicellulose and physically-chemically linked with lignin, the enzymes access to the raw cellulose matrix is difficult [8]. Thus, acid and alkali pretreatments are typically performed to separate the hemicellulose and lignin polymers from the cellulosic material resulting in a cellulose-enriched solid and in a preliminary release of sugars [7].

However, from an industrial-scale perspective, the use of pretreatments causes several economic and environmental disadvantages. Particularly, the use of an acid pretreatment step results in high costs associated with acid recovery, the purchase of corrosive-resistant equipment, the removal of inhibitory compounds for both enzymatic hydrolysis and fermentation, and the management of wastewater [9]. Indeed, in the context of bioethanol production, Procentese et al. [10] estimated that the cost of pretreatment accounts for approximately

* Corresponding author.
E-mail address: maer@igt.sdu.dk (M. Errico).

https://doi.org/10.1016/j.bej.2023.109044
Received 6 June 2023; Received in revised form 21 July 2023; Accepted 22 July 2023
Available online 25 July 2023

Nomenclature

BSG	Brewers' Spent Grain.
CM	Chrastil's model.
df1,2	degrees of freedom.
DM	Dry matter.
EL	enzyme loading, $mL_{enz}\ g^{-1}_{dry\ BSG}$.
$[E]_0$	initial enzyme concentration, g L^{-1}.
[G]	glucose concentration, g L^{-1}.
$[G]_0$	initial glucose concentration, g L^{-1}.
$[G]_\infty$	equilibrium glucose concentration, g L^{-1}.
k	Chrastil's model rate constant, L g^{-1} h^{-1}.
k_{MCM}	modified Chrastil's model rate constant, L g^{-1} h^{-1}.
LS	liquid to solid ratio, $g_{liq}\ g^{-1}_{solid}$.
MCM	modified Chrastil's model.
MS	Mean sum of Squares.
$m_{Dry\ BSG}$	mass of dry BSG introduced in the reactor, g.
m_{liq}	mass of buffer solution, g.
n	Chrastil's model structural diffusion resistance constant, dimensionless.
n_{MCM}	modified Chrastil's model structural diffusion resistance constant, dimensionless.
p	number of factors.
SS	Sum of Squares.
SGP	Soluble Glucose Polysaccharides.
$[S]_0$	initial substrate concentration, g L^{-1}.
S_θ	normalised sensitivity index, dimensionless.
t	time, h.
T	temperature, °C.
V_{enz}	enzyme volume injected in the reactor, mL.
V_R	reaction volume, L.
X_i	i-th independent variable.
X_j	j-th independent variable.
x_G	potential glucose mass fraction in dried BSG determined by its characterization, without considering soluble glucose polysaccharides, -
$x_{G,enz}$	glucose mass fraction in enzyme blend, -
Y_G	estimated glucose yield, % $g_{Glucose}\ g^{-1}_{Dry\ BSG}$.
$\widehat{Y}_G$	estimated glucose yield, % $g_{Glucose}\ g^{-1}_{Dry\ BSG}$.
Y_G^{exp}	experimental glucose yield, % $g_{Glucose}\ g^{-1}_{Dry\ BSG}$.
$\widehat{\beta}_0$	regression model intercept.
$\widehat{\beta}_i$	linear coefficient of i-th variable.
$\widehat{\beta}_{ii}$	quadratic coefficient of i-th variable.
$\widehat{\beta}_{ij}$	coefficient of interaction between i-th and j-th variables.
θ	generic Chrastil's model parameter.
$\theta_{est}-$	estimated generic Chrastil's model parameter.
ρ_{enz}	enzyme density, g mL^{-1}.

0.13–0.17 € per liter of ethanol, which represents at least 25 % of the competitive selling price of the final product of about 0.6 € per liter of ethanol. Hence, though the effect of pretreatment methods of lignocellulosic biomass is to increase the enzymatic digestibility of the raw materials, it may not be economically attractive. Enzymatic saccharification of dried BSG that has not been subjected to further treatments such as acid or alkali treatments, referred to as untreated BSG, could therefore be an interesting strategy to reduce costs.

Optimization and kinetic characterization of BSG enzymatic hydrolysis are two crucial issues. Mussatto et al. [11] and Rojas-Chamorro et al. [12] investigated the influence of process variables on enzymatic hydrolysis of pretreated BSG and optimized the process.

Moreover, the feasibility to produce bioethanol from the enzymatic hydrolysate of untreated BSG has recently been published [13] using a one-pot system, consisting of an initial enzymatic saccharification phase followed by ethanolic fermentation in the same reactor proving that is possible to obtain an ethanol yield comparable to other studies where the BSG was pretreated. However, the optimization and the kinetic characterization of untreated BSG saccharification has not yet been reported.

The present work investigates the effect of enzyme loading, temperature and substrate loading on enzymatic hydrolysis of untreated BSG with regard to glucose yield. Response Surface Methodology (RSM), is used to find the optimal process conditions.

The kinetic study of the reaction is known to be challenging due to the complexity of the heterogeneous BSG matrix that deviates from the classical Michaelis-Mentenś model [14,15]. A deep understanding of the hydrolysis kinetics is crucial for bioreactors design, as it provides knowledge of the functionality between operational variables and the conversion rates of polysaccharides into fermentable sugars and allows predicting the dynamics of such a system. To this purpose, Chrastil [16] introduced the model (CM) reported in Eq. 1, which was adopted to assess the mass transfer characteristics of BSG enzymatic hydrolysis:

$$[G] = [G]_\infty \left[1 - \exp(-k[E]_0 t)\right]^n \quad (1)$$

Based on the experimental data, the kinetic parameter *k*, which is a rate constant proportional to the diffusion coefficient of the enzyme in the substrate matrix [10], *n* which refers to the structural diffusion resistance dependent on the steric structure of the system [15], and the equilibrium glucose concentration $[G]_\infty$ were estimated. However, the estimation of CM's parameters can be misleading as there may be correlations between them resulting in a less accurate estimation and wide parameter confidence intervals. This leads to an unreliable characterization of the process kinetics. Therefore, a modified Chrastil model (MCM) is proposed in this work to describe the temporal profile of glucose during BSG enzymatic saccharification. The knowledge of the model parameters provides a deeper understanding of the dynamic behavior of untreated BSG enzymatic saccharification, which to the best of the authors' knowledge, has not yet been reported.

2. Materials and methods

2.1. Raw material

The BSG was provided by Vestfyen Brewery, Assens, Denmark. It was initially stored at −4 °C and then oven-dried at 90 °C in five cycles of 2 h until a constant weight was reached. The BSG solid content was 25 % wt. The dried solid was stored at room temperature for further experiments.

2.2. Enzymatic hydrolysis

Cellic ® CTec2 (>1000 Biomass Hydrolysis Units, density of 1.209 g/L; Novozymes, Denmark) was used to perform the enzymatic hydrolysis. This enzyme complex comprises a blend of α-cellulase, β-glucosidases and hemicellulases. The reaction environment was a sodium citrate buffer 0.05 M containing 0.04 % w/v sodium azide to remove microbial contaminants, the reaction volume was 500 mL, and the pH was 4.8. A straight-blade impeller was used, and the agitation speed was set at the impeller motors' minimum value, 280 rpm. Three experimental runs were carried out to observe the transient behavior of the system. After the system reached the target temperature, the enzyme was added. Samples were taken at the beginning of the run, after 30 min,

then at intervals of 1 h after the first 60 min, 2 h after the first 5 h up to 9 h of reaction, and then the last samples were taken after 21, 24, and 30 h.

For the optimization, 14 experiments were performed. However, samples were taken only at the beginning and at the end of the run, specified as a reaction time of 24 h. For both the transient behavior and optimization experiments, the glucose content in the commercial enzyme mixtures was quantified by HPLC and subtracted from the glucose concentrations obtained from each sample [17]. The measured glucose mass fraction in the enzyme blend was 0.261 ± 0.006 [13], equivalent to 0.32 ± 0.008 g mL^{-1}.

2.3. Analytical methods

National Renewable Energy Laboratory (NREL) standard laboratory analytical procedures for biomass analysis were used to characterize the composition of untreated BSG [18,19]. These procedures were performed in triplicate. Regarding the enzymatic hydrolysis, aliquots of 3 mL of the slurry (liquid+solid) were sampled from the reactor, pre-filtered through 0.4 μm and then through 0.20 μm filters (Sartorius, Germany), before being analyzed by HPLC to quantify the glucose concentration. The HPLC setup (Ultimate 3000, Thermo Fisher) was equipped with a Phenomenex Rezex RHM-Monosaccharide H+ (8 %) analyzing column with a refractive index detector (Dionex Softron GmbH, Germany). The operative temperature was 79 °C and the mobile phase was ultrapure water (0.6 mL/min). The glucose retention time was identified using standard solutions and its concentration was quantified through calibration curves. The limits of the concentration interval were [0.1–50 g/L] with a coefficient of determination equal to 0.9993. A significant amount of solubilized glucose polysaccharide (i.e., SGP) derived from unconverted starch and free glucose monomers was identified in the slurry before the enzyme was added. The SGP mass fraction was determined by HPLC quantification of a liquid sample withdrawn 30 min after the system reached the reaction temperature and before adding the enzyme.

2.4. Statistical tools

2.4.1. Experimental design and process optimization

The effect of enzyme loading (EL), liquid-to-solid ratio (LS), and temperature (T) on the glucose yield was investigated. The experimental glucose yield was calculated according to Eq. 2:

$$Y_G^{exp} = \frac{[G]_{(t=24h)} \times V_R - V_{enz}\rho_{enz}x_{G,enz}}{m_{DM}} \times 100 \quad (2)$$

Box–Behnken design with two replications at the central point was used to develop the Design of Experiments (DoE). This design provides three levels for each factor coded as [− 1,0,1]. The coded and uncoded values of all the regressor variables are shown in Table 1.

The temperature range was chosen according to the optimal conditions recommended in the enzyme information sheet [20] and analogous studies where the same enzyme was used on lignocellulosic substrates [21,22]. The solid-to-liquid ratio was defined according to the studies of Pinheiro et al. [23] and Wilkinson et al. [24] on BSG processing while the enzyme loading was defined according to the experimental plan proposed by Mussatto et al. [11].

Response Surface Methodology (RSM), coupled with Analysis of Variance (ANOVA) was used to develop a reliable functionality between the response variable and the factors under analysis. Minitab™ was used to fit the data to the polynomial function reported in Eq. 3 and optimize the process [25]:

$$\hat{Y}_G = \hat{\beta}_0 + \sum_{i=1}^{p}\hat{\beta}_i X_i + \sum_{i=1}^{p}\hat{\beta}_{ii}X_i^2 + \sum_{i=1}^{p}\sum_{j=i+1}^{p}\hat{\beta}_{ij}X_iX_j \quad (3)$$

The regression model of Eq. 3 was then validated by experimentally assessing the glucose yield of the corresponding estimated optimum point. Stepwise backward elimination was used to find the significant parameters to fit the experimental data [26]. The significance level was set as 5 % for all the hypothesis tests carried out. The variance explained by the model was assessed with the coefficient of determination R^2.

Table 1
Experimental design for the enzymatic hydrolysis.

Run	T [°C]		LS* [g liquid/g_{DM}]		EL [mL/g_{DM}]	
	real	coded	real	coded	real	coded
1	45	–1	25	0	0.214	1
2	45	–1	25	0	0.043	–1
3	55	1	35	–1	0.128	0
4	45	–1	35	–1	0.128	0
5	50	0	35	–1	0.043	–1
6	50	0	15	1	0.043	–1
7	45	–1	15	1	0.128	0
8	55	1	15	1	0.128	0
9	55	1	25	0	0.214	1
10	50	0	15	1	0.214	1
11	55	1	25	0	0.043	–1
12	50	0	35	–1	0.214	1
13	50	0	25	0	0.128	0
14	50	0	25	0	0.128	0

* Liquid to Solid ratio value equal to 15 [g of liquid per gram of dry BSG] has been coded as 1 because is the condition corresponding to the highest substrate loading. Analogously −1 was the coded value attributed to 35 [g of liquid per gram of dry BSG] corresponding to the lowest substrate loading condition.

2.4.2. Kinetic modeling

Enzyme-substrate kinetics are usually described using the Michaelis-Menten equation [27]. Nevertheless, often the kinetic parameters obtained from the regression yield unrealistic values. Furthermore, the Michaelis-Menten equation assumes the system to be homogeneous. Indeed, the heterogeneous nature of the process is firstly due to the presence of both liquid and solid phases. In addition, the substrate (i.e., cellulose) is strongly held inside the lignin matrix. In such a case, the reaction may show mass transfer limitation due to the enzyme diffusing through the complex structure of the lignocellulosic material to reach the cleavage point on the substrate. Further, according to Chrastil [16], the problem when doing regression on time-dependent data based on product concentration arises from the assumption of pseudo-steady-state equilibrium between the enzyme and substrate and not including the thermodynamic equilibrium of the complete set of reactions occurring in the system. Taking these factors into account for batch processes where the enzyme transport into the matrix is rate limiting, Chrastil [16] arrived at the diffusion-limiting kinetic model shown in Eq. 1. According to this model, when the term n tends to the unity, diffusion resistances are negligible, while if it is comprised between 0 and 1, the system is limited by diffusion resistance [10]. Nevertheless, some modifications have been introduced to consider its original formulation limitations. Firstly, Eq. 1 assumes that the initial glucose concentration is zero. This assumption does not represent the experimental conditions in this paper, meaning that it was necessary to add the contribution of the glucose concentration at the beginning of the experimental run, $[G]_0$.

The original formulation of the CM can be corrected as shown in Eq. 4:

$$[G] = [G]_0 + ([G]_\infty - [G]_0)\left[1 - \exp(-k_{CM}[E]_0 t)\right]^n \quad (4)$$

Eq. 4 is now a three-parameter ($[G]_\infty$, k, n) non-linear model, whose parameters estimation may be challenging due to their strong correlation. This leads to wide confidence intervals and thus large uncertainty in the parameter values determined. It was reasonably assumed that $[G]_0$ was numerically equal to the sum of glucose concentration associated with the soluble glucose polysaccharide (SGP), solubilized during temperature system conditioning prior to the introduction of the enzyme,

and the glucose concentration associated with the inoculation of the enzyme blend. Therefore, under the mentioned assumptions the term $([G]_\infty - [G]_0)$ corresponds to the amount of glucose generated during the reaction.

In order to propose a modified version of the CM, it was introduced the maximum mass of glucose per unit of reaction volume that theoretically can be generated from the process $[S]_0$ (i.e the mass of cellulosic glucose in dry BSG per unit of reaction volume). This term is expected to be higher than $[G]_\infty - [G]_0$ and its value was experimentally determined according to Eq. 5.

$$[S]_0 = \frac{x_G m_{liq}}{LS \ V_R} \tag{5}$$

$[S]_0$ is related to the amount of glucose potentially releasable since x_G was obtained by multiplying the glucan fraction in dry BSG times 1.11, that is the stoichiometric factor for its hydration upon hydrolysis [23].

In order to take into account that only a fraction of such cellulosic glucose can effectively be obtained at the end of the reaction, $[S]_0$ was raised to the power of n, and substituted to $([G]_\infty - [G]_0)$ as shown in Eq. 6.

$$\left([G]_\infty - [G]_0\right) = [S]_0^{\,n_{MCM}} \tag{6}$$

In general, high recalcitrant lignocellulosic systems satisfy the inequality $n < 1$. Procentese et al. [10] for apple pomace, evaluated n between 0.41 and 0.63 depending on the pretreatment used. For corn hub, Ayeni et al. [14] evaluated the same parameter in the range of 0.37–0.65, depending on the enzyme concentration used. Consequently, it can be inferred that the relation $[S]_0^{\,n} < [S]_0$ holds as well (if $n > 1$, this model loses its physical meaning). Therefore, a MCM is proposed to fit the glucose concentration as a function of time. In this way, the resulting equation contains two parameters, namely n_{MCM} and k_{MCM}. By substituting Eq. 6 into Eq. 4 it is possible to obtain the MCM shown in Eq. 7.

$$[G] = [G]_0 + [S]_0^{\,n_{MCM}} \left[1 - \exp(-k_{MCM}[E]_0 t)\right]^{n_{MCM}} \tag{7}$$

It is important to emphasize that the n parameter in the MCM retains the same meaning as in the classical CM (Eqs. 1,4). The parameters of both CM and MCM were determined by fitting the experimental data with Eq. 4 and Eq. 7, respectively using the Statistical and Machine Learning toolbox of MATLAB R2022b®. The confidence interval was evaluated for each parameter to assess the reliability of the estimation for both models. The level of confidence was set equal to 95 %. Moreover, ANOVA tests were carried out to evaluate the adequacy of the regression models. All experiments relevant to the dynamic analysis were performed at 55 °C under three different BSG and enzyme loadings according to the experimental conditions reported in Table 2. The operational conditions adopted for the kinetic analysis of enzymatic hydrolysis lie within the range of values studied during optimization. Specifically, the enzyme loading for the first and second experimental tests reported in Table 2 are the corresponding highest and lowest value of the DoE respectively calculated for the highest biomass loading. The third run corresponds to the highest enzyme load referred to the lowest biomass loading. Experiments were performed in duplicate, such that it was possible to fit the average product concentration for each reaction time and assess the model's Lack of Fit (LoF) by performing the LoF test [28].

Table 2
Experimental conditions for the analysis of the enzymatic saccharification dynamic behavior analysis. Temperature was set at 55 °C for all three runs.

Run	Enzyme concentration [g/L]	LS [g_{liq}/g_{DM}]	$[S]_0$ [g/L]
1	12.75	15	16.37
2	2.56	15	16.37
3	5.46	35	7.02

3. Results and discussion

3.1. Raw BSG composition

BSG's chemical composition varies according to barley variety, harvest time, malting and mashing conditions, and the quality and type of adjuncts added in the brewing process [1]. Therefore, BSG characterization is not trivial, and many factors may significantly affect the BSG composition. Table 3 shows the composition amounts as weight percentage of dry BSG used in the experiments (% wt. DM). It is shown that the uncertainty is slightly less than 10 % for each sugar, which highlights how BSG characterization is influenced by a high degree of uncertainty. In addition, many other factors like time of conservation and drying conditions may affect the BSG composition.

According to Table 3, almost 63 % of the total dry weight of BSG is structural sugars. Particularly, glucose content is relatively high compared to the values reported by Mussatto et al. [7], while the total lignin content shown in this work (15.4 %wt) is noticeably lower. Interestingly the mass fraction of acid-soluble and insoluble lignin is also lower compared to that of other lignocellulosic materials like barley straw, corn stover or sweet sorghum [17]. A low lignin content is expected to enhance the enzymatic access to cellulose chains, as lignin acts as a barrier that hinders the enzymatic transport to the cleave bonds of the substrate. On the other hand, the ash content obtained is similar to the one reported in other studies [17,29].

3.2. Enzymatic saccharification of untreated BSG

The influence of temperature, solid loading, and enzyme loading on the glucose yield for the enzymatic hydrolyzation of dried BSG are reported in Table 4.

Glucose yield in the enzymatic hydrolysates varied in a narrow range, from 8.0 (run 11) to 11.4 $g_{glucose}/100g_{DM}$ (run 10). As expected, the enzyme loading strongly affects the performance of the process since, in most cases, the higher the amount of enzyme, the higher the amount of glucose released at a given time. Nevertheless, the ninth run showed a relatively low performance even though the enzyme loading was at the highest value tested. In this case, the temperature was also the highest within the DoE, which may have caused degradation of the enzyme and/or glucose itself, leading to a lower glucose yield. Hence, the negative effect of high temperature can easily be seen as only run 8 shows a $\widehat{Y}_G$ greater than 10 $g_{glucose}/100g_{DM}$ among those run at 55 °C.

It is worth mentioning that a small amount of pentose sugars (xylose and arabinose) was detected in the enzymatic hydrolysates due to the hemicellulase content in the enzymatic blend. However, since this work focuses on glucose generation, their quantity was not considered in terms of process performances but they are reported as sugar yield in the Supplementary Material.

Run 10 was the experiment with the highest glucose yield,

Table 3
Composition of BSG, expressed as average value ± standard deviation, and correspondent analytical method.

Component	Content (%wt DM)	Method used
Ash	3.6 ± 0.1	[18]
Glucose	26.8 ± 2.2	[19]
of which SGP	2.24 ± 0.01	
Hemicellulosic sugars	35.8 ± 1.6	[19]
Xylose	24.0 ± 2.0	[19]
Arabinose	11.8 ± 1.0	[19]
Acid soluble lignin	9.9 ± 1.6	[19]
Acid insoluble lignin	5.5 ± 1.6	[19]
Others[a]	18.4	[–]
Total mass	100	

[a] Other components, obtained by difference, may include protein and extractives.

Table 4
Glucose yields obtained from the BSG enzymatic hydrolysis.

Run	T[°C]	LS[g_{liq}/g_{DM}]	EL [mL_{enz}/g_{DM}]	$\hat{Y}_G$ [$g_{glucose}/100g_{DM}$]
1	45	25	0.214	10.61
2	45	25	0.043	8.23
3	55	35	0.128	9.31
4	45	35	0.128	9.47
5	50	35	0.043	9.07
6	50	15	0.043	9.79
7	45	15	0.128	11.30
8	55	15	0.128	10.16
9	55	25	0.214	9.60
10	50	15	0.214	11.43
11	55	25	0.043	8.04
12	50	35	0.214	10.63
13	50	25	0.128	10.19
14	50	25	0.128	10.02

corresponding to 43 % of the potentially releasable glucose. This value is slightly higher than reported by Michelin and Teixeira [30], where the enzymatic hydrolysis of untreated BSG under similar conditions to those applied in this work showed a cellulose conversion equal to 37 %. This is probably this is due to the lower content of lignin in the raw BSG used in this study.

3.3. Estimation of model parameters and process optimization

Glucose yield ($\hat{Y}_G$) expressed as g of glucose per 100 g of dry mass was chosen to optimize the saccharification process. Temperature (T), enzyme loading (EL) and liquid-to-solid ratio (LS) were the factors chosen to model the process and predict the optimal hydrolysis condition at which $\hat{Y}_G$ reaches its maximum value. RSM was used to identify the optimal conditions. Backward stepwise elimination was implemented to evaluate the statistical significance of the individual regression coefficients in Eq. 3. For each step, Extra Sum of Squares statistical test was employed with a significance level of 0.05 [28]. During each step the regression sum of squares related to the partial model (without the parameter under investigation), SSR_p, and the regression sum of squares related to the full model (comprising the parameter under evaluation), SSR_f, were calculated. In this way, for each generical step, it was possible to compute $SSR_{ex} = SSR_f - SSR_p$ (i.e. extra sum of squares), the increase in regression sum of squares due to the inclusion of the extra parameter to a model that comprises all the parameters that have not been eliminated in the previous steps. Table 5 shows the results of the ANOVA.

The test shows that the first- and second-degree terms for all three independent variables were significantly different from zero leading to Eq. 8:

$$\hat{Y}_G = -42.4 + 2.257T - 0.3193LS + 24.95EL - 0.02319T^2 + 0.00534LS^2 - 56.5EL^2 \quad (8)$$

Hence, a second-order polynomial can be used to model the glucose yield. The coefficient of determination is 94.98 %. According to the R^2 value the model was highly predictive for the glucose yield, and all the factorial variables had a strong influence on the final sugar concentration. Fig. 1 shows the resulting contour plot of the regression model with the experimental results. According to the regression equation, the optimal condition is found for a temperature of 48.6 °C, a liquid-solid ratio of 15 g_{liq}/g_{DM}, and an enzyme loading of 0.220 mL_{enz}/g_{DM}.

As expected, enzyme loading was the variable with the highest impact, as seen in (Fig. 1-b; 1-c). A negative quadratic term for the enzyme loading implies the possible existence of a maximum optimum concentration that may correspond to substrate saturation of the enzyme. This means that using an amount of enzyme higher than the optimal one (i.e., 0.220 mL_{enz}/g_{DM}) does not improve the process performance though it could affect the dynamic behavior. The optimal temperature is found to be close to 50 °C, in agreement with the optimal conditions stated in the information sheet for the enzyme [20]. Moreover, the optimal LS ratio lies in the minimum extreme of the experimental domain (15 g_{liq}/g_{DM} or 6.7 % w/w), which means that a higher substrate loading led to higher glucose yields. This may be due to a higher soluble glucose concentration favoured by a greater biomass loading [10]. This consideration holds for low to medium solid loadings, indeed considering 15 % w/w as high biomass loading, it was proved that the resulting high viscosity of the slurry limits the effectiveness of the enzymatic hydrolysis due to an uneven enzyme distribution and ineffective slurry mixing, among other phenomena [31].

3.4. Model validation

Once the optimal condition was found through the RSM technique, the reaction was carried out at the predicted optimal condition in order both to maximize the glucose yield and to validate the regression equation. Fig. 2 shows the results of the validation by plotting the optimal value and its standard deviation in the surface response previously developed.

As can be seen, the model well predicts the behavior of the Cellic CTec2 enzymatic complex. Indeed, the experimental glucose recovery

Table 5
Analysis of variance for enzymatic hydrolysis results.

Source	df1	df2	SS	MS	F-Value	$F_{0.05}$ (df1,df2)	P-Value
Regression	6	7	12.3776	2.06293	22.07	3.8660	$<10^{-4}$
T	1	7	1.0175	1.01752	10.89	5.5914	0.013
LS	1	7	1.2847	1.28470	13.74	5.5914	0.008
EL	1	7	1.5408	1.54083	16.48	5.5914	0.005
T^2	1	7	1.0757	1.07568	11.51	5.5914	0.012
LS^2	1	7	0.9122	0.91218	9.76	5.5914	0.017
EL^2	1	7	0.5451	0.54514	5.83	5.5914	0.046
T × LS	1	6	nr	nr	3.4411	5.9874	0.113
T × EL	1	5	nr	nr	3.28	6.6079	0.130
LS × EL	1	4	nr	nr	0.02	7.7086	0.885
Residuals	7		0.6543	0.09348			

nr: not reported

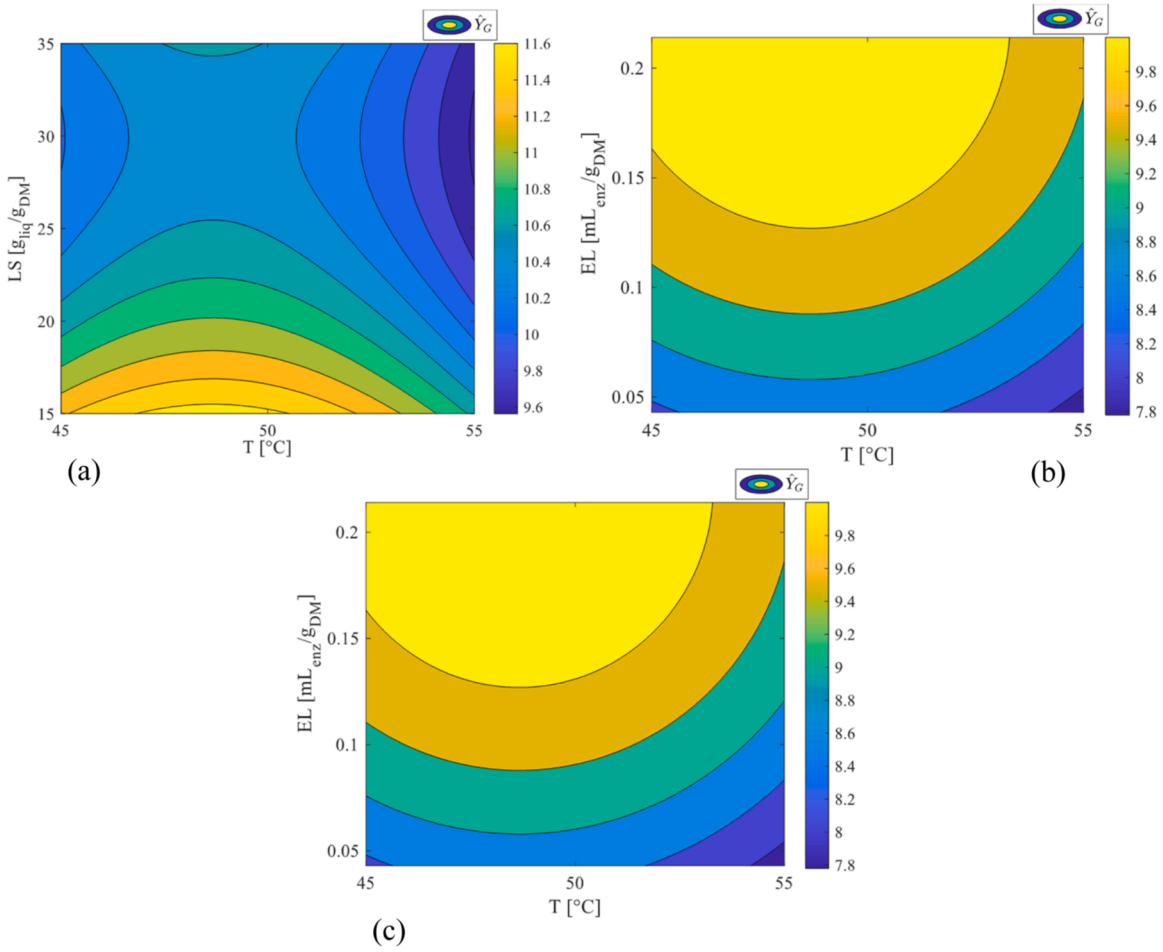

Fig. 1. Response contour plot for the glucose yield as a function of temperature and liquid-to-solid ratio where EL was at the optimal value of 0.220 [$mL_{enz}g_{DM}^{-1}$], (a), enzyme loading and temperature where the liquid-solid ratio was set equal to the optimal value of 15 [$g_{liq}g_{DM}^{-1}$] (b), liquid-solid ratio and enzyme loading at the optimal temperature of 48.6 °C (c).

under the optimal condition was 11.71 ± 0.09 $g_{glucose}/100g_{DM}$ while the predicted value was 11.68 $g_{glucose}/100g_{DM}$. Such value corresponds to a glucose conversion of 44 % respect to the theoretical value, which doubles the value of about 22 % reported by Mussatto et al. [7] when the enzymatic hydrolysis of untreated BSG was not optimized.

It is important to remember that four variables are involved in the analysis, namely temperature, enzyme loading, and liquid-solid ratio as regressor variables, and glucose yield as the dependent one. Therefore, the variables were individually fixed at the optimal condition to construct the three plots presented in Fig. 2.

3.5. Reaction kinetics assessment

The second phase of the study aims at characterizing the kinetic behavior of Cellic CTec2 converting glucan chains in the BSG solid matrix to glucose. The application of the CM and the MCM may be an efficient approach to fit the glucose trend to the reaction time. Table 6 shows the kinetic parameters and the relative confidence interval determined by fitting the experimental values. For this analysis, enzyme and solid loading were expressed in g/L and wt% respectively.

Both models, the CM and MCM were evaluated to describe the dynamic behavior of the system under investigation. The CM model includes an additional parameter, $[G]_\infty$, compared to the MCM model meaning that one would expect that the MCM would have a lower R^2 than the CM. On the other hand, the addition of an extra parameter does not necessarily lead to a significant improvement in the model's performance. In fact, results shown in Table 6 indicate that both models were able to adequately describe the dynamic behavior of the system. Still, the CM model has wider confidence intervals for the estimated parameters. In particular, the use of the MCM model resulted in a reduced error margin given by the confidence interval width of approximately 40 % points for the estimated k and 7 % points for the estimated n, thus resulting in a more reliable estimation of the kinetic parameters. It is worth noting that, compared to the CM,

the MCM parameters resulted in a narrower confidence interval. Moreover, the MCM parameters lie within the corresponding interval of confidence obtained by fitting the data with the CM. Overall, the kinetic constant varied in the range of almost one order of magnitude (0.006–0.040), while the parameter n varied between 0.33 and 0.5. Variations of enzyme and solid loading had similar effects on the parameter estimation for both models, meaning that the following considerations apply to both the MCM and the CM. Concerning the parameter n, its value was below 0.6 meaning that the steric effect of the system is important [15]. It is seen that n is lower when the solid loading decrease and enzyme loading is relatively higher (run 3). This phenomenon can be explained by the saturation of the cleavage sites of the substrate by the enzyme. Indeed, Carrillo et al. [32] suggested that the enzyme is initially adsorbed on the fibre surface forming one single layer, such that the surplus enzyme forms additional layers, hindering the diffusion enzymes through the substrate fibres. Regarding the parameter k, the results show that k is larger at lower enzyme loadings (run 2) when substrate concentration is kept constant. Carrillo et al. [32] also highlighted that hydrolysis inhibition phenomena related to

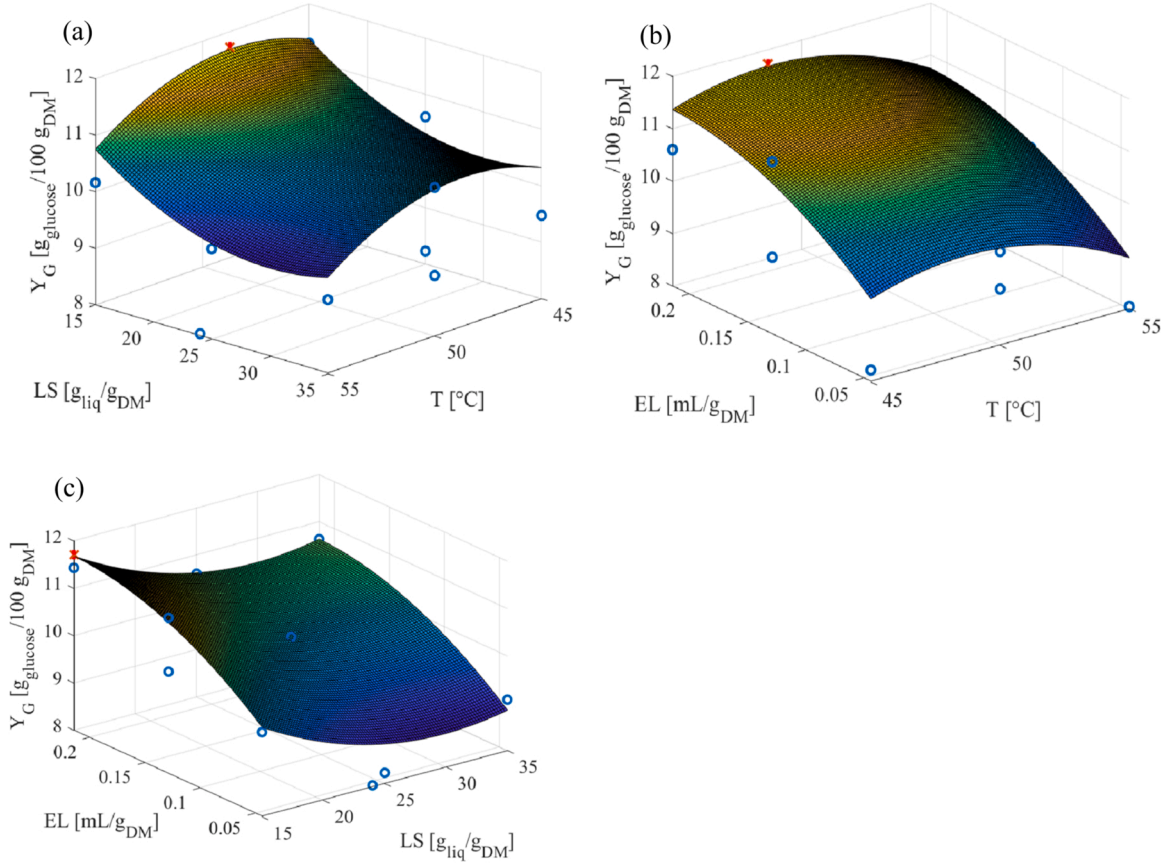

Fig. 2. Results of model validation for BSG enzymatic hydrolysis by Cellic CTec2. Response surface plot for the glucose yield as a function of T and LS where EL was set equal to 0.220 [$mL_{enz}g_{DM}^{-1}$], (a); EL and T where LS was set equal to 15 [$g_{liq}g_{DM}^{-1}$] (b); LS and EL where T was set equal to 48.6 °C (c).

Table 6
Kinetic parameters relevant to enzymatic hydrolysis of untreated BSG with Cellic CTec2. Operative temperature was 55 °C.

			CM				MCM		
Run	Enzyme concentration [g/L]	Solid loading [% wt]	$[G]_\infty$ [g/L]	k [L/ (g h)]	n [-]	R^2	k_{MCM} [L/ (g h)]	n_{MCM} [-]	R^2
1	12.75	6.7	10.2±0.2	0.008±0.003	0.50±0.09	0.995	0.006±8•10^{-4}	0.44±0.02	0.994
2	2.56	6.7	6.3±0.3	0.040±0.03	0.50±0.1	0.988	0.034±7 •10^{-3}	0.46±0.02	0.987
3	5.46	2.8	4.9±0.2	0.015±0.009	0.34±0.07	0.992	0.017±2 •10^{-3}	0.33±0.02	0.992

product formation occur at high enzyme concentrations, reducing the catalytic activity of the enzyme system. The end-product inhibition caused by high glucose concentration is widely reported [11] and it probably explains the results obtained in this work according also to the glucose concentration profiles reported in Fig. 3. Finally, a further analysis is given to the equilibrium glucose concentration assessed in the classic CM. It is worth underlining that all three tests were performed with three different enzyme concentrations, resulting in three different initial glucose concentrations. Therefore, for the sake of comparison the amount of glucose produced during the reaction is assessed by subtracting the initial glucose concentration associated to the introduction of the commercial enzyme. According to the model estimations, 5.69 g/L of glucose were produced once the final yield was reached in the first experiment, while 5.37 g/L and 2.91 g/L of produced glucose were the estimated as final asymptotic values of [G] for the second and the third runs respectively. Results obtained in the first two runs, which have the same solid loading, suggest that after 30 h, the system has nearly reached the final yield and show that changes in enzyme concentration have a low influence on the final glucose concentration, meaning that the amount of enzyme introduced in the system only affects the process dynamic behavior. A lower final glucose concentration estimated in the third trial is related to a lower substrate loading.

ANOVA tests were performed to evaluate models' performances. Tests for the significance of regression and lack of fit test were carried out in order to assess the goodness of fit of the investigated kinetic models. For the test for significance of regression, the null hypothesis under investigation is H_0: $[G]_\infty = 0$, $k = 0$, $n = 0$ while the alternative hypothesis is H_1: at least one parameter is different from zero. Regarding the lack of fit test, the null hypothesis is H_0: the relationship assumed to fit the experimental data is reasonable (i.e. there is no lack of fit), while the alternative one is H_1: The relationship assumed to describe data behavior is not adequate (i.e. there is a lack of fit).

The results of the ANOVA test reported in Table 7 clearly show that the models are adequate for describing experimental data. Regarding the test for the significance of regression the observed F-value is greater than the critical value, with a significance level equal to 5 % meaning that the null hypothesis is rejected and the significance of the regression is statistically confirmed for both the CM and the MCM. On the other hand, the lack of fit test resulted in an observed F-value that is smaller than the critical value with a significance level equal to 5 % meaning that the null hypothesis is statistically confirmed for both the CM and the MCM. Fig. 3 shows experimental data fitted by CM and MCM, both of

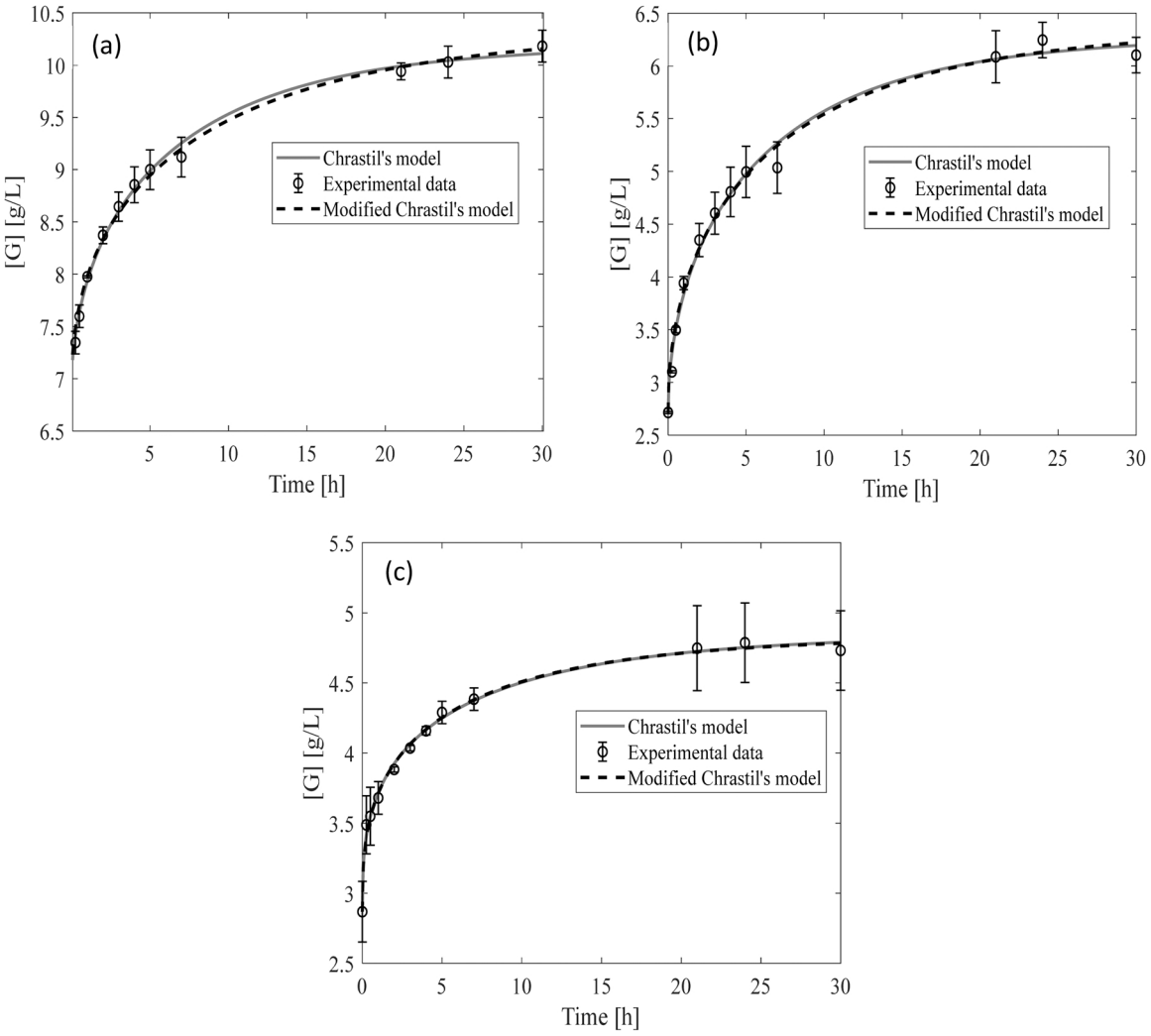

Fig. 3. Evolution of glucose concentration during BSG enzymatic hydrolysis simulated by CM and MCM compared with the experimental data in correspondence of three different experimental conditions: dry solid loading equal to 6.7 % wt and enzyme concentration equal to 12.75 g/L (a), dry solid loading equal to 6.7 % wt with an enzyme concentration equal to 2.56 g/L (b), and a dry solid loading equal to 2.8 % and enzyme concentration equal to 5.46 g/L (c).

Table 7
Analysis of variance for Chrastil's model and modified Chrastil's model.

	CM					MCM				
Source	DF	SS	MS	F-Value	P-Value	DF	SS	MS	F-Value	P-Value
Regression										
Run 1	2	9.103	4.552	882	~0	1	8.844	8.844	1474	~0
Run 2	2	10.74	5.368	354	~0	1	10.541	10.541	753	~0
Run 3	2	2.293	1.147	597	~0	1	2.319	2.319	1160	~0
Residuals										
Run 1	9	0.047	0.005			10	0.058	0.006		
Run 2	9	0.137	0.015			10	0.143	0.014		
Run 3	9	0.017	0.002			10	0.018	0.002		
Lack of fit										
Run 1	9	0.451	0.050	0.231	0.980	10	0.085	0.009	0.305	0.960
Run 2	9	0.175	0.019	0.644	0.738	10	0.176	0.018	0.582	0.794
Run 3	9	0.152	0.017	0.0624	0.999	10	0.025	0.003	0.057	~ 1
Pure error										
Run 1	9	0.250	0.028			9	0.250	0.028		
Run 2	9	0.273	0.030			9	0.273	0.030		
Run 3	9	0.398	0.044			9	0.398	0.044		

which evidently describe the transient behavior of enzymatic saccharification of untreated BSG by means of Cellic CTec2 well.

It is interesting to analyze the final glucose concentration reached after long reaction times. The values obtained in each run are significantly lower than the theoretical glucose concentration that would be expected at equilibrium. Indeed, after subtracting the initial glucose

amount in the commercial enzyme blend from the final glucose concentration, it was found that only 32 %, 29 % and 36 % of the potentially obtainable glucose was produced in run 1, run 2 and run 3 respectively. Michelin and Teixeira [30] suggested that the availability of cellulose to enzymatic attack is strongly affected by the inner fibrillar and rigid structure combined with a high crystallinity of cellulose. Hall et al. [33] reported that the initial hydrolysis rate of cellulose linearly decreases with the crystallinity of this polysaccharide. Hence, crystallinity and structure rigidity may have acted as a barrier that completely hindered enzyme access to the largest fraction of cellulose present in the reactive system, preventing achieving complete substrate conversion. The comparison of the kinetic parameters obtained have also been extended to other studies in which CM was used for hydrolyses of biomasses other than BSG. Similar results were observed when, for the same enzyme complex, the biomass lignin content was comparable. Further details are available in the Supplementary Material.

3.6. Sensitivity analysis

To evaluate the impact of the parameters on CM and MCM performances a sensitivity analysis was performed. In this analysis, each parameter ranged between two limits (from 0 up to twice the estimated values reported in Table 6) and it was assessed the variation of the final glucose concentration estimated by the model. Fig. 4 shows the trend of the estimated glucose concentration corresponding to 30 h of saccharification by varying each individual parameter, and the estimated parameter value is highlighted (diamond marker). Only plots related to the first run are reported for brevity, while the analysis of runs 2 and 3 is reported in the Supplementary Material. Regarding the CM, Fig. 4-a reports the influence of the reaction rate constant on the estimated glucose concentration. It is evident that an increase in the rate constant corresponds to an increase of the final glucose concentration up to a critical value equal to the value obtained by regression and reported in Table 6. The CM appears to be not sensitive to an increase of the k value beyond this value. Regarding the n parameter (Fig. 4-b), it can be clearly seen that it does not significantly affect the final glucose concentration. This result complies with the CM: when the glucose concentration is approaching the final value, the exponential term is close to zero, meaning that the whole term raised to the power of n is approximately one. Furthermore, the final glucose concentration approaches $[G]_\infty$ as expected, justifying the linear dependence between the response variable and this parameter. For the MCM, the same conclusion is reached when analyzing the effect of k_{MCM} on the estimated final glucose concentration. In the MCM, an increase of the parameter n_{MCM} reflects a slower glucose generation through the exponential term along with a higher steady state product concentration, related to an increase of the contribution of the maximum allowable glucose concentration term. Therefore, since steady-state glucose concentration is considered in this analysis, the exponential term can be reasonably neglected, and the only significant effect of an individual variation of n_{MCM} to $[G]_{(t=30h)}$ concentration is related to $[S]_0^{n_{MCM}}$ (Fig. 4-e).

In order to further explore the model parameters influence on the glucose concentration it is useful to assess the trend of the sensitivity index for each individual parameter at different reaction times. The normalized sensitivity index $S_\theta(t)$ of the θ parameter was evaluated according to Eq. 9 [34], discretized by central finite difference, as proposed by Peri et al. [35]:

$$S_\theta(t) = \frac{\theta_{est}}{[G](t)} \left.\frac{d[G](t)}{d\theta}\right|_{\theta_{est}} \quad (9)$$

Here, θ_{est} is the parameter estimated by the model. This makes it possible to study the effect of the variation of a single parameter in the neighborhood of the estimated value on the glucose concentration for each hydrolysis time. The sensitivity index behavior with reaction time is depicted in Fig. 5. Again, only results relevant to the first run are reported for both models. Plots related to CM highlight that the sensitivity of $[G]_\infty$ exponentially increases over time until the normalized sensitivity index reached 1. This result agrees with the previously mentioned conclusion regarding the final glucose concentration $[G]_\infty$ (Fig. 4-c). Interestingly, the sensitivity index relative to k shows a different behavior: during the first reaction hour, the model output becomes more sensitive to changes in k until a peak is reached. Thereafter, the model

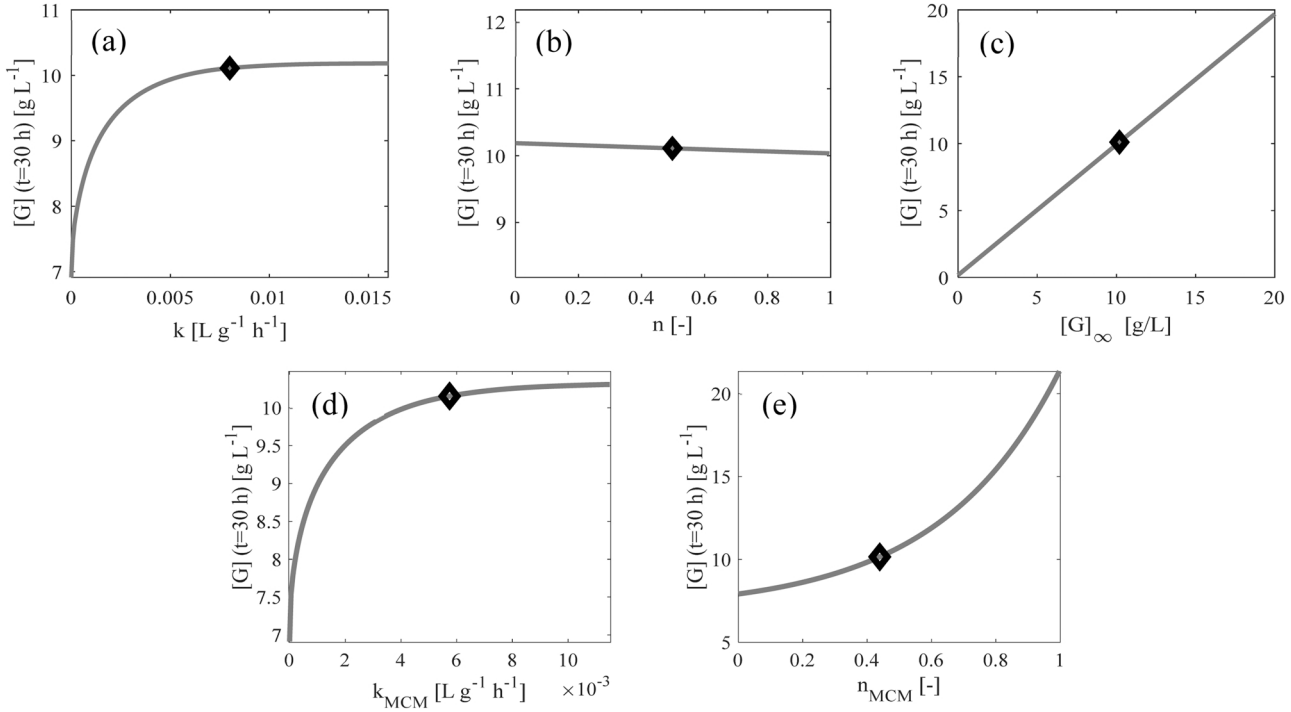

Fig. 4. Effect of model parameters on final glucose concentration (t = 30 h) for the Chrastil's model (a,b,c), and modified Chrastil's model (d,e). Diamond points refer to the nominal parameter value obtained from the non-linear regression.

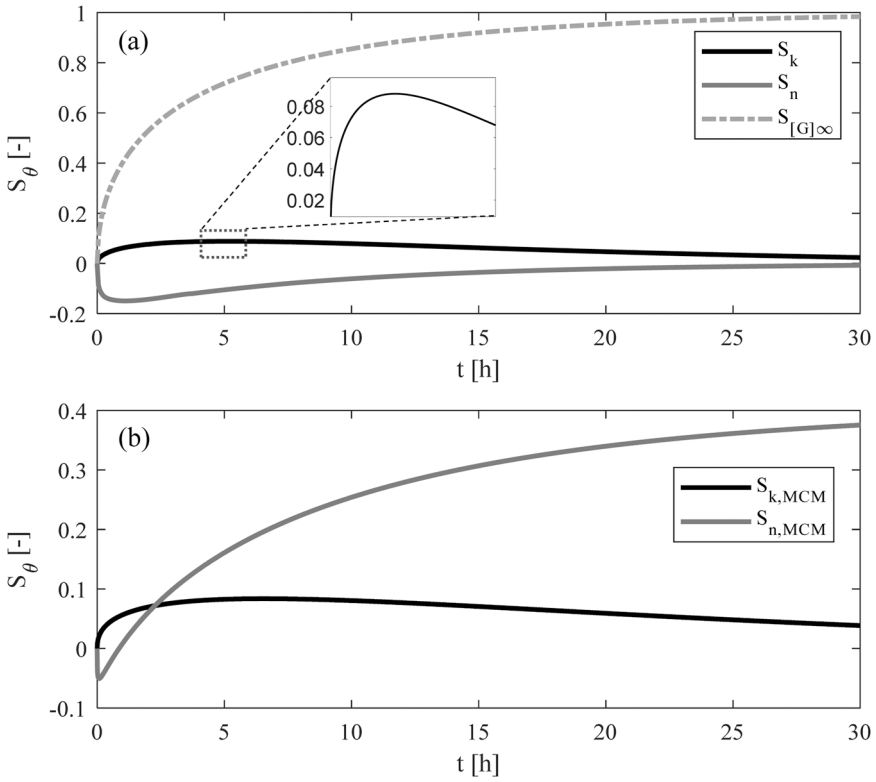

Fig. 5. Variation of the sensitivity index with respect to time for the CM (a) and MCM (b).

begins to show little or no sensitivity to this parameter. Similar behavior is observed with the *n* parameter, but the sign of the sensitivity index is the opposite. This means that an individual increase in the kinetic constant will result in an increase in the extent of cellulose saccharification, whereas an individual increase in the structural diffusion resistance constant will reduce the estimated glucose concentration until zero sensitivity is reached. In particular, a higher *n* value gives rise to more sluggish glucose concentration-time curves. Although the latter statement may seem contradictory with the definition of the structural diffusion resistance constant given above, it is important to specify that this analysis evaluates how individual parameters affect the dynamic performance of the system without considering the influence of a combined variation of two or more parameters to the time-dependent glucose concentration profile. Indeed, results obtained by Carrillo et al. [32] with regard to CM parameters for enzymatic saccharification of wheat straw can explain this complex behavior. In their work, the enzymatic hydrolysis of untreated wheat straw resulted in small values of the structural diffusion resistance constant and low final values for the glucose concentration, corresponding to a faster achievement of the final constant glucose yield. On the other hand, hydrolysis of alkali-pretreated wheat straw allowed the system to reach a higher value for the final glucose concentration but showed a slower response as a consequence of the increase in *n* related to a reduced steric hindrance of the biomass [32]. In addition to this, it is widely reported that such structural modification increases the structural diffusion resistance constant *n* [10,15].

Fig. 5-a shows that the glucose concentration dependency of reaction time estimated by CM is strongly sensitive to the final glucose concentration except in the first few minutes of the enzymatic process. This result interestingly links with the results reported in Fig. 3, where it was observed that, in the best case only 36 % of the potentially available glucose was hydrolyzed at the end of the run. Thus, it is reasonable to state that steric effects that prevent the enzyme to access into a great fraction of cellulose are correlated to final glucose concentration and a modification of the biomass matrix may guarantee higher final glucose concentrations. Concerning the parameter sensitivity index for MCM (Fig. 5-b) as a function of reaction time, the trend of $S_{k,MCM}(t)$ is the same as that of S_k (t) while, on the contrary, an interestingly different behavior was obtained for $S_{n,MCM}(t)$. Particularly, as reaction time increases, the sensitivity index of n_{MCM} changes sign: starting from zero, $S_{n,MCM}(t)$ decreases until a negative minimum is reached. Thereafter, the sensitivity index for the *n* parameter monotonically increases. This means that during the first stages of enzymatic hydrolysis, an increase in n_{MCM} results in a decrease in the extent of glucose production. After approximately one hour of reaction, $S_{n,MCM}(t)$ changed in sign, indicating that in a later stage of reaction, similar increase in n_{MCM} results in a greater glucose concentration. This highlights the efficiency of MCM at describing the transient behavior of enzymatic hydrolysis of untreated lignocellulosic biomass: the n_{MCM} parameter combines the negative effect of *n*, which results in a slower response with increasing values (if the other parameters are kept constant) with the positive effect given by an increment of $[G]_\infty$, when mass transfer limitations within the reacting system are reduced. Thus, it is possible to regress time data by means of a model that is both simpler in terms of the number of parameters and adequate at describing the process dynamics. In fact, from a visual inspection of the time profile for the glucose concentration reported in other works it is evident that, when comparing two runs from which two remarkably different *n* values were obtained, the experiment with the smaller *n* showed a higher glucose concentration at the early reaction times along with a lower glucose concentration in the later ones and vice versa [15,32]. In conclusion, it is important to emphasize that when analyzing the product concentration time profile in lignocellulosic systems, the final product concentration and the parameters that take into account the steric properties of the system cannot be assessed separately but have to be evaluated jointly.

4. Conclusions

The conversion process of the untreated BSG cellulosic fraction to fermentable sugars is a promising approach that can reduce the amount

of this by-product landfilled. Since fermentation represents one of the most explored valorization routes, it is crucial to maximise the hydrolysis yield of fermentable sugars. At the same time the characterization of the saccharification process through a simple reaction kinetic model is of paramount importance for a possible large-scale application. The response surface method was used to optimize the BSG saccharification process by developing a polynomial model which describes the functionality that links the glucose yield to the enzyme loading, substrate loading, and temperature. At the optimal conditions, a glucose yield of 44 % with respect to the theoretical one was obtained. A novel modelling approach based on the classic Chrastil's model is proposed to fit the experimental glucose concentration obtained at different reaction times. The model resulted simple and able to fit the experimental data satisfactorily, ensuring a more precise parameter estimation in comparison to the classical Chrastiĺs model. When BSG underwent different operating conditions, the kinetic behavior of the system and the kinetic model parameters changed. A sensitivity analysis, such as the one performed in this study, opens a comprehensive understanding of the impact of these variations on the parameter estimation and their effect on the glucose concentration for each reaction time.

CRediT authorship contribution statement

Leonardo Sibono: Methodology, Investigation, Validation, Formal analysis, Data Curation, Writing – Original Draft, **Stefania Tronci**: Conceptualization, Methodology, Writing – Review & Editing, **Ron Hajrizaj**: Investigation, Writing – Review & Editing, **Knud V. Christensen**: Conceptualization, Methodology, Resources, Writing – Review & Editing, **Massimiliano Errico**: Conceptualization, Methodology, Investigation, Writing – Review & Editing, Project administration Funding acquisition, **Massimiliano Grosso**: Conceptualization, Methodology, Formal analysis, Validation, Writing – Review & Editing.

Declaration of Competing Interest

The authors declare that they have no known competing financial interests or personal relationships that could have appeared to influence the work reported in this paper.

Data Availability

Data will be made available on request.

Acknowledgments

This project has received funding from the European Union's Horizon 2020 research and innovation programme under the Marie Sklodowska-Curie grant agreement No 778168.

The authors are thankful to Novozymes A/S for providing the enzymes and to Vestfyen Brewery for the BSG.

Appendix A. Supporting information

Supplementary data associated with this article can be found in the online version at doi:10.1016/j.bej.2023.109044.

References

[1] S.I. Mussatto, G. Dragone, I.C. Roberto, Brewers' spent grain: generation, characteristics and potential applications, J. Cereal Sci. 43 (1) (2006) 1–14, https://doi.org/10.1016/j.jcs.2005.06.001.

[2] Jan Conway, 2022 ⟨https://www.statista.com/statistics/270275/worldwide-beer-production/⟩ (accessed 04 July, 2023).

[3] S.I. Mussatto, M. Fernandes, I.M. Manchilha, I. Roberto, Effects of medium supplementation and pH control on lactic acid production from brewer's spent grain, Biochem. Eng. J. 40 (2008) 437–444, https://doi.org/10.1016/j.bej.2008.01.013.

[4] D.S. Tang, G.M. Yin, Y.Z. He, S.Q. Hu, B. Li, L. Li, H.L. Liang, D. Borthakur, Recovery of protein from brewer's spent grain by ultrafiltration, Biochem. Eng. J. 48 (2009) 1–5, https://doi.org/10.1016/j.bej.2009.05.019.

[5] M.P. Fernandez, J.F. Rodriguez, M.T. Garcia, A. de Lucas, I. Gracia, Application of supercritical fluid extraction to brewerś spent grain management, Ind. Eng. Chem. Res. 47 (2008) 1614–1619, https://doi.org/10.1021/ie0708529.

[6] C. Sakdaronnarong, N. Srimarut, N. Lucknakhul, N. Na-songkla, W. Jonglertjunya, Two-step acid and alkaline ethanolysis/alkaline peroxide fractionation of sugarcane bagasse and rice straw for production of polylactic acid precursor, Biochem. Eng. J. 85 (2014) 49–62, https://doi.org/10.1016/j.bej.2014.02.003.

[7] S.I. Mussatto, M. Fernandes, A.M.F. Milagres, I.C. Roberto, Effect of hemicellulose and lignin on enzymatic hydrolysis of cellulose from brewer's spent grain, Enzym. Microb. Technol. 43 (2) (2008) 124–129, https://doi.org/10.1016/j.enzmictec.2007.11.006.

[8] W. Liao, Z. Wen, S. Hurley, Y. Liu, C. Liu, S. Chen, Effects of hemicellulose and lignin on enzymatic hydrolysis of cellulose from dairy manure, Appl. Biochem. Biotechnol. - Part A Enzym. Eng. Biotechnol. 124 (2005) 1017–1030, https://doi.org/10.1385/ABAB:124:1-3:1017.

[9] J.C. Solarte-Toro, J.M. Romero-García, J.C. Martínez-Patiño, E. Ruiz-Ramos, E. Castro-Galiano, C.A. Cardona-Alzate, Acid pretreatment of lignocellulosic biomass for energy vectors production: a review focused on operational conditions and techno-economic assessment for bioethanol production, Renew. Sustain. Energy Rev. 107 (2019) 587–601, https://doi.org/10.1016/j.rser.2019.02.024.

[10] A. Procentese, M.E. Russo, I. Di Somma, A. Marzocchella, Kinetic characterization of enzymatic hydrolysis of apple pomace as feedstock for a sugar-based biorefinery, Energies 13 (5) (2020) 1051, https://doi.org/10.3390/en13051051.

[11] S.I. Mussatto, G. Dragone, M. Fernandes, A.M.F. Milagres, I.C. Roberto, The effect of agitation speed, enzyme loading and substrate concentration on enzymatic hydrolysis of cellulose from brewer's spent grain, Cellulose 15 (5) (2008) 711–721, https://doi.org/10.1007/s10570-008-9215-7.

[12] J.A. Rojas-Chamorro, I. Romero, J.C. López-Linares, E. Castro, Brewer's spent grain as a source of renewable fuel through optimized dilute acid pretreatment, Renew. Energy 148 (2020) 81–90, https://doi.org/10.1016/j.renene.2019.12.030.

[13] L. Sibono, S. Tronci, M. Grosso, R. Hajrizaj, M. Errico, Brewerś spent grain to bioethanol through a hybrid saccharification and fermentation process, Chem. Eng. Trans. 99 (2023), https://doi.org/10.3303/CET2399002.

[14] A.O. Ayeni, O. Agboola, M.O. Daramola, B. Grabner, B.A. Oni, D.E. Babatunde, J. Evwodere, Kinetic study of activation and deactivation of adsorbed cellulase during enzymatic conversion of alkaline peroxide oxidation-pretreated corn cob to sugar, Korean J. Chem. Eng. 38 (1) (2021) 81–89, https://doi.org/10.1007/s11814-020-0667-2.

[15] B. Pratto, R.B.A. de Souza, R. Sousa, A.J.G. da Cruz, Enzymatic hydrolysis of pretreated sugarcane straw: kinetic study and semi-mechanistic modeling, Appl. Biochem. Biotechnol. 178 (7) (2016) 1430–1444, https://doi.org/10.1007/s12010-015-1957-8.

[16] J. Chrastil, Enzymic product formation curves with the normal or diffusion limited reaction mechanism and in the presence of substrate receptors, Int. J. Biochem. 20 (7) (1988) 683–693, https://doi.org/10.1016/0020-711X(88)90163-2.

[17] J.A. Rojas-Chamorro, C. Cara, I. Romero, E. Ruiz, J.M. Romero-Garcia, S. I. Mussatto, E. Castro, Ethanol production from brewers' spent grain pretreated by dilute phosphoric acid, Energy Fuels 32 (4) (2018) 5226–5233, https://doi.org/10.1021/acs.energyfuels.8b00343.

[18] A. Sluiter, B. Hames, R. Ruiz, C. Scarlata, J. Sluiter, Determination of ash in biomass - NREL/TP-510-42622, Natl. Renew. Energy Lab (2005). ⟨https://www.nrel.gov/docs/gen/fy08/42622.pdf⟩.

[19] A. Sluiter, B. Hames, R. Ruiz, C. Scarlata, J. Sluiter, D. Templeton, D. Crocker, Determination of structural carbohydrates and lignin in biomass - NREL/TP-510-42618, Natl. Renew. Energy Lab. (2008). ⟨http://www.nrel.gov/docs/gen/fy13/42618.pdf⟩.

[20] Novozyme. Cellic Ctec2 information sheet, ⟨http://www.shinshu-u.ac.jp/faculty/engineering/chair/chem010/manual/Ctec2.pdf⟩; 2022 [accessed 02/06/2023].

[21] F.R. Paz-Cedeno, J.M. Carceller, S. Iborra, R.K. Donato, A.F. Ruiz Rodriguez, M. A. Morales, E.G. Solorzano-Chavez, I.U. Miranda Roldan, A. Veloso de Paula, F. Masarin, Stability of the Cellic CTec2 enzymatic preparation immobilized onto magnetic graphene oxide: assessment of hydrolysis of pretreated sugarcane bagasse, Ind. Crops Prod. 183 (2022), 114972, https://doi.org/10.1016/j.indcrop.2022.114972.

[22] H. Østby, A. Várnai, R. Gabriel, P. Chylenski, S.J. Horn, S.W. Singer, V.G.H. Eijsink, Substrate-dependent cellulose saccharification efficiency and LPMO Activity of Cellic CTec2 and a cellulolytic secretome from *Thermoascus aurantiacus* and the impact of H_2O_2-producing glucose oxidase, ACS Sustain. Chem. Eng. 10 (2022) 14433–14444, https://doi.org/10.1021/acssuschemeng.2c03341.

[23] T. Pinheiro, E. Coelho, A. Romaní, L. Domingues, Intensifying ethanol production from brewer's spent grain waste: Use of whole slurry at high solid loadings, N. Biotechnol. 53 (2019) 1–8, https://doi.org/10.1016/j.nbt.2019.06.005.

[24] S. Wilkinson, K.A. Smart, D.J. Cook, A comparison of diluted acid- and alkali-catalyzed hydrothermal pretreatments for bioethanol production from brewersśpent grains, J. Am. Soc. Brew. Chem. 72 (2014) 143–153, https://doi.org/10.1094/ASBCJ-2014-0327-02.

[25] D.C. Montgomery. Design and Analysis of Experiments, 10th edition.,, Wiley,, 2020.

[26] R.R. Hocking, The analysis and selection of variables in linear regression, Biometrics 32 (1976) 1–49, https://doi.org/10.2307/2529336.

[27] R. Sirohi, J.P. Pandey, R. Goel, A. Singh, U.C. Lohani, A. Kumar, Two-stage enzymatic hydrolysis for fermentable sugars production from damaged wheat grain

starch with sequential process optimization and reaction kinetics, Starch 73 (2020) 1–9, https://doi.org/10.1002/star.202000082.
[28] D.M. Bates, D.G. Wattes, Nonlinear Regression Analysis and Its Applications, Wiley,, 2007.
[29] M.G. Moran-Aguilar, I. Costa-Trigo, M. Calderón-Santoyo, J.M. Domínguez, M. G. Aguilar-Uscanga, Production of cellulases and xylanases in solid-state fermentation by different strains of Aspergillus niger using sugarcane bagasse and brewery spent grain, Biochem. Eng. J. 172 (2021), https://doi.org/10.1016/j.bej.2021.108060.
[30] M. Michelin, J.A. Teixeira, Liquid hot water pretreatment of multi feedstocks and enzymatic hydrolysis of solids obtained thereof, Bioresour. Technol. 216 (2016) 862–869, https://doi.org/10.1016/j.biortech.2016.06.018.
[31] Shiva, F. Climent Barba, R.M. Rodriguez-Jasso, R.K. Sukumaran, H.A. Ruiz, High-solids loading processing for an integrated lignocellulosic biorefinery: effects of transport phenomena and rheology – a review, Bioresour. Technol. 351 (2022), 127044, https://doi.org/10.1016/j.biortech.2022.127044.
[32] F. Carrillo, M.J. Lis, X. Colom, M. López-Mesas, J. Valldeperas, Effect of alkali pretreatment on cellulase hydrolysis of wheat straw: Kinetic study, Process Biochem. 40 (10) (2005) 3360–3364, https://doi.org/10.1016/j.procbio.2005.03.003.
[33] M. Hall, P. Bansal, J.H. Lee, M.J. Realff, A.S. Bommarius, Cellulose crystallinity - a key predictor of the enzymatic hydrolysis rate, FEBS J. 277 (6) (2010) 1571–1582, https://doi.org/10.1111/j.1742-4658.2010.07585.x.
[34] T. Lenhart, K. Eckhardt, N. Fohrer, H.G. Frede, Comparison of two different approaches of sensitivity analysis, Phys. Chem. Earth Parts A/B/C. 27 (9) (2002) 645–654, https://doi.org/10.1016/S1474-7065(02)00049-9.
[35] S. Peri, S. Karra, Y.Y. Lee, M.N. Karim, Modeling intrinsic kinetics of enzymatic cellulose hydrolysis, Biotechnol. Prog. 23 (2007) 626–637, https://doi.org/10.1021/bp060322s.